COMMUNICATION

Investigation of the dynamic nature of 1,2-oxazines derived from peralkylcyclopentadiene and nitrosocarbonyl species†

Victoria K. Kensy,[a] Gregory I. Peterson,‡[a] Derek C. Church,[a] Neal A. Yakelis[b] and Andrew J. Boydston*[a]

We have investigated the reversible hetero-Diels–Alder reaction of 1,2-oxazines derived from a peralkylcyclopentadiene and a series of nitrosocarbonyl dienophiles. The nature of the dienophile was found to impart broad tunability to the dynamic character of the oxazine adducts. The reversibility was also observed in polymeric systems. The fidelity of the reaction and tunable sensitivity toward elevated temperature and water signify potential applications in the development of dynamic covalent materials or delivery systems for small molecule payloads.

Fig. 1 Generalized depiction of the reversible HDA reaction of nitrosocarbonyls.

Introduction

For decades, the hetero-Diels–Alder (HDA) reaction of nitroso-carbonyl species has been utilized as a versatile synthetic transformation for production of 1,2-oxazines (Fig. 1).[1–7] Attractive aspects include the potential for regio- and stereo-controlled introduction of nitrogen and oxygen into carbon frameworks, and ample opportunities for downstream manipulation of the *N*-substituted oxazine. In a subset of examples of 1,2-oxazine applications, the ready reversibility of the HDA reaction was targeted as a means to control *in situ* generation of highly reactive nitrosocarbonyl moieties. For example, King, Miyata, and Toscano have highlighted the potential to use this cycloreversion for generation of HNO, a purported therapeutic, presumably following hydrolysis of the nitrosocarbonyl intermediate.[8–14]

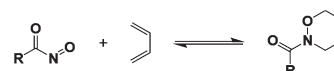More recently, the dynamic HDA reaction of nitrosocarbonyls has been applied in the design of advanced polymeric architectures and functional materials. A key example from Read de Alaniz and coworkers demonstrated application of nitrosocarbonyl HDA reactions to prepare block copolymers *via* highly efficient polymer chain end coupling.[15] In their report, reactive nitrosocarbonyl dienophiles were generated *in situ* at polymer chain ends either by oxidation of hydroxamic acids or cycloreversion of 9,10-dimethylanthracene-based adducts. In the presence of a complementary cyclopentadiene-terminated polymer, efficient chain end coupling was accomplished.

Inspired by this movement toward applications in the polymer field, we considered integration of polymer chain end coupling and nitrosocarbonyl hydrolysis to enable controlled deconstruction of block copolymers.[16] For this purpose, the 1,2-oxazine moiety was employed as a thermally labile trigger. Upon thermolysis, subsequent hydrolysis of the nitrosocarbonyl intermediate initiated a controlled depolymerization sequence leading to deconstruction of a self-immolative polymer block. Clearly, the "click-like" nature of the HDA reaction, tunable cycloreversion of oxazines, diverse reactivity of nitrosocarbonyl species, and overall structural modularity provide a powerful combination for advances in polymer and materials designs.

We became interested in the potential applications of polymers and network materials bearing high densities of oxazine moieties. One may envision, for example, taking advantage of robust dynamic covalency to access covalent adaptable networks as has been demonstrated for Diels–Alder and HDA adducts.[17–21] Such systems display broad tunability with regard to stimuli-responsiveness and overall materials properties, stemming largely from the modularity of the diene and dienophile building blocks. On the other hand, controlled

[a]Department of Chemistry, University of Washington, Seattle, Washington 98195, USA. E-mail: ajb1515@uw.edu
[b]Department of Chemistry, Pacific Lutheran University, Tacoma, Washington 98447, USA

This journal is © The Royal Society of Chemistry 2016

Org. Biomol. Chem., 2016, **14**, 5617–5621 | 5617

breakdown of oxazine-rich materials could enable controlled release of HNO. HNO generation has received a lot of attention in recent years due to its purported use as a treatment of cardiovascular diseases and as an anticancer agent.[22–26] Notably, the breadth of potential applications place disparate demands on the reactivity of the oxazine and constituent nitrosocarbonyl species (high fidelity cycloaddition/cycloreversion *versus* hydrolytic instability) while maintaining a need for retro-HDA reactions to take place at moderate temperatures. To further explore the chemical space and potential applications of oxazine-based systems, we have investigated the reversibility and robustness of a series of oxazines relevant to polymer-oriented applications. Herein, we describe our investigations of the reactivity of oxazines derived from a series of nitrosocarbonyl dienophiles and a peralkylcyclopentadiene. Particular focus is placed upon comparative analysis of the reversibility of the HDA reaction as a function of nitrosocarbonyl structure, and overall fidelity of the cycloaddition/cycloreversion equilibrium *versus* deleterious side reactions.
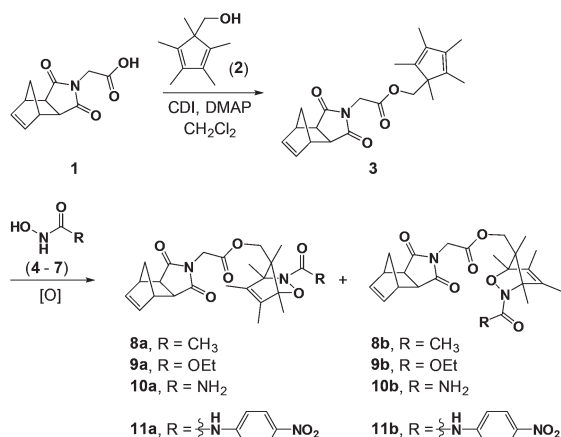
Results and discussion

Motivated by potential downstream applications in the development of functional polymeric materials, we targeted oxazines that were based upon readily polymerizable norbornene frameworks.[27] Additionally, we centered upon cyclopentadiene-based oxazines to provide an attractive starting point for balance between stability and reversibility of the HDA adducts. Toward this end, coupling of carboxylic acid 1 and alcohol 2 in the presence of carbonyldiimidazole (CDI) provided ester 3 in 70% isolated yield (Fig. 2). This pivotal intermediate was then used to prepare a series of oxazines *via* HDA reaction with nitrosocarbonyl species generated *in situ*.[1,28–30]

We initially evaluated the use of CuCl/pyridine to catalyze the nitrosocarbonyl formation. Although good yields of 11 were achieved *via* oxidation of 7 in the presence of 3, analogous reactions with coupling partners 4–6 were met with limited success. Turning instead to tetrabutylammonium periodate (TBAP) as a stoichiometric oxidant remedied the situation, providing the corresponding oxazines 8–10 in good to excellent yields. Notably, each oxazine was isolated as a mixture of what appeared to be a roughly 3 : 1 ratio of two diastereomers (each racemic).

Separation of the isomers by standard chromatographic techniques was unsuccessful. However, we found that slow vapour diffusion of diethyl ether into solutions of 10 in CH_2Cl_2 produced single crystals suitable for X-ray analysis. We were able to separate crystals that were ultimately found to be individual diastereomers 10a and 10b (Fig. 3), which can be viewed as *anti* and *syn* isomers, respectively. With small quantities of each diastereomer of 10 at hand, we were able to obtain a discrete ^{1}H NMR spectrum for each. From these, we identified 10a as the major diastereomer produced in the initial mixture of products. The CH_3 groups indicated in Fig. 3 proved to be useful diagnostic handles for ^{1}H NMR analyses and tracking of *anti* and *syn* isomers for oxazines 8, 9, and 11 by analogy to 10.

We next turned toward probing the dynamic nature of each oxazine. Specifically, each set of isomers was heated in DMSO-d_6 (15 mM) and monitored by ^{1}H NMR spectroscopy. In each case, the initial mixture contained a roughly 3 : 1 ratio of diastereomers, which equilibrated to a roughly 1 : 1 ratio over time. At ambient temperature, no observable isomerization took place for any of the oxazines over the course of several hours. When heated at 37 °C (Fig. 4, top), we observed gradual equilibration of the diastereomers with strong dependence upon the nature of the nitrosocarbonyl component. For example, oxazine 8 did not appear to reach equilibrium even

Fig. 2 Synthesis of norbornene-tethered oxazine isomers. In each case, reactions proceeded to 100% conversion as judged by TLC.

Oxazine	Oxidant	Time (h)	Isolated Yield
8	TBAP	2	64%
9	TBAP	2.5	97%
10	TBAP	3	88%
11	CuCl, pyridine	18	70%

Oxidation Conditions

8a, R = CH₃   8b, R = CH₃
9a, R = OEt   9b, R = OEt
10a, R = NH₂   10b, R = NH₂
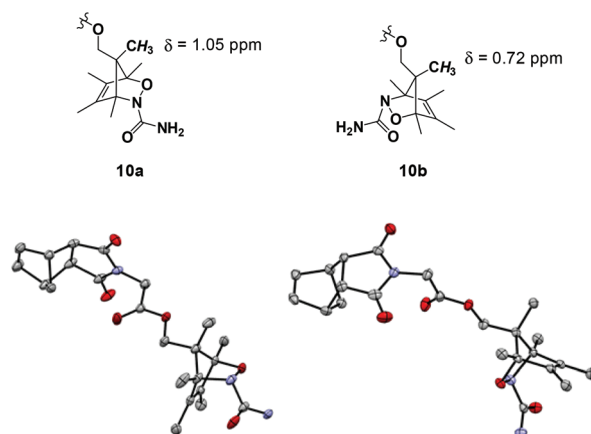11a, R = (NHC₆H₄NO₂) 11b, R = (NHC₆H₄NO₂)

Fig. 3 Molecular structures obtained *via* single crystal X-ray analysis of (left) 10a, and (right) 10b. Ellipsoids drawn at the 50% probability level, protons removed for clarity.

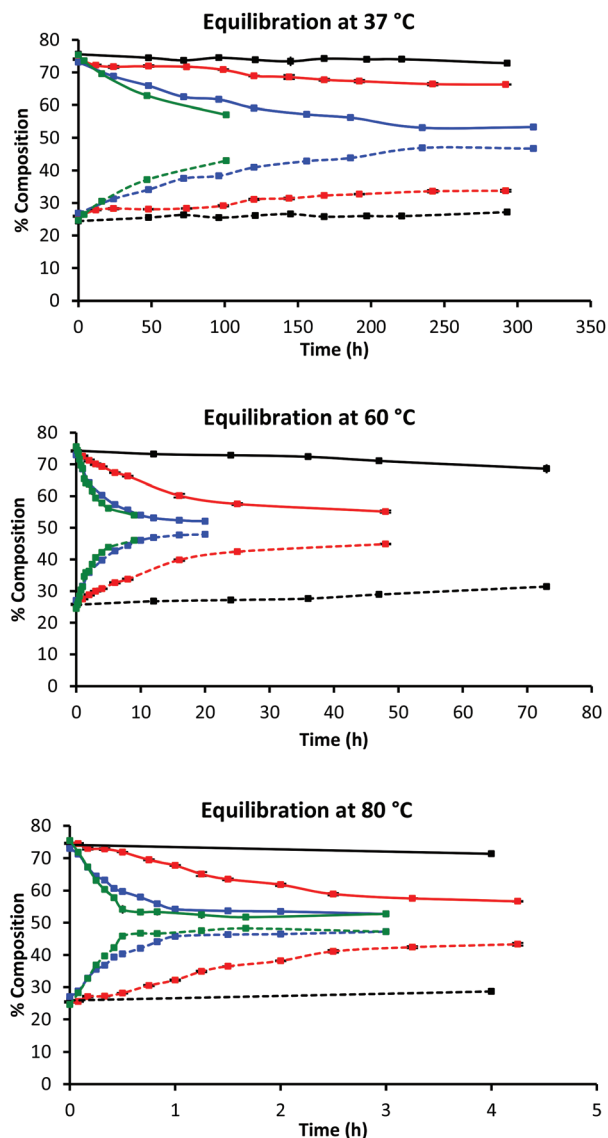δ = 1.05 ppm (10a)   δ = 0.72 ppm (10b)

Fig. 4 Equilibration of oxazines in DMSO-d_6. Solid line = isomer A, dashed line = isomer B. Black = **8**, red = **9**, blue = **10**, green = **11**. Data points are an average of three runs, errors bars = one standard deviation, lines are for visual aid only.[31] Percent composition refers to the ratio of isomers A and B.

ible isomerization over the course of several days, whereas changes in the diastereomeric ratios for **10** and **11** appeared to have ceased after a few hours. Further increase in the temperature to 80 °C (Fig. 4, bottom) resulted in full equilibration within minutes for **10** and **11** (50 and 25 min, respectively), whereas the composition of **8** continued to show gradual change over the course of several hours (see ESI† for extended plots).

As stated previously, the oxazine retro-HDA reaction releases nitrosocarbonyl species, which have the potential to undergo hydrolysis, dimerization, or ene reactions.[32] These deleterious reactions were not observed to any appreciable extent in the experiments represented in Fig. 4 despite prolonged reaction times and no special precautions being taken to dry the DMSO solvent. To explore the oxazine reactivity in aqueous environment, we examined each of the oxazines at 60 °C in a 30% D_2O/DMSO-d_6 mixture, which was the maximum D_2O content at which each of the oxazines remained soluble at room temperature. Each oxazine mixture was monitored by ^{1}H NMR spectroscopy for 156 h. Oxazines **8** and **9** showed no loss of oxazine content and isomerization rates similar to those observed in DMSO-d_6. In contrast, examination of oxazine **10** revealed a small amount of cyclopentadiene **3** (4.5%) developing over the course of the experiment (Fig. 5, top). Presumably, the formation of **3** can be ascribed to
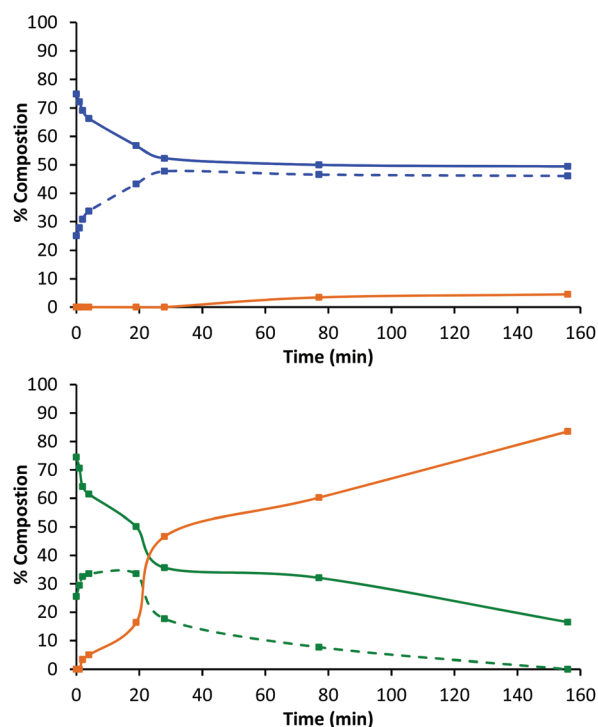

Fig. 5 Equilibration and hydrolysis of oxazines in D_2O/DMSO-d_6 at 60 °C.[31] Solid line = isomer A, dashed line = isomer B. (top) Oxazine **10** in blue, cyclopentadiene **3** in orange. (bottom) Oxazine **11** in green, cyclopentadiene **3** in orange. Data points are an average of two runs, lines are for visual aid only. Percent composition refers to the fraction of each species relative to the total sum of isomer A, isomer B, and **3**.

within 12 d at 37 °C, indicating much slower isomerization than oxazines bearing more electron donating substituents (*cf.* **9**–**11**). Oxazine **9** appeared to isomerize more rapidly than **8**, but also continued to show gradual change in the ratio of isomers up to 12 d. The hydroxyurea-derived systems (**10** and **11**) were found to approach equilibrium at the highest relative rates. The facile isomerization, particularly of **10** and **11**, at 37 °C suggests to us that these platforms may be suitable for incorporation into dynamic covalent networks or related materials that become active under biological conditions.

The general trend in isomerization rate (**8** < **9** < **10** < **11**) was preserved at the higher temperatures as well (Fig. 4). At 60 °C (Fig. 4, middle), the least reactive oxazine (**8**) displayed discern-

This journal is © The Royal Society of Chemistry 2016

Org. Biomol. Chem., 2016, **14**, 5617–5621 | **5619**

hydrolysis of the intermediate nitrosocarbonyl species. When oxazine **11** was examined under the aqueous reaction conditions, we found nearly complete loss of both oxazine isomers and concomitant formation of **3** (Fig. 5, bottom). Collectively, these results confirm that the oxazine moiety can be structurally tuned toward either robust dynamic behaviour or controlled degradation.

Encouraged by the results from the small molecule oxazine studies, we next explored whether the dynamic nature would remain consistent within related polymeric systems. Toward this end, we synthesized **poly(11)** *via* ring-opening metathesis polymerization (ROMP) using a third-generation Grubbs catalyst (Fig. 6).[33] Specifically, monomer **11** was reacted with the Ru-based initiator (35 : 1 initial monomer to initiator ratio) in CH$_2$Cl$_2$ at 0 °C for 3 h, at which point full consumption of monomer was confirmed by ^{1}H NMR analysis. Following termination of the polymerization with ethyl vinyl ether, filtration through alumina/Celite, and isolation by precipitation of the polymer into methanol, we obtained **poly(11)** in 57% isolated yield. Analysis of **poly(11)** by ^{1}H NMR spectroscopy and gel-permeation chromatography (GPC) indicated intact oxazines (3 : 1 ratio of isomers), a weight-average molecular weight (M_w) of 30.0 kDa, and a molecular weight dispersity ($Đ$) of 1.05.

With **poly(11)** at hand, we then monitored the isomerization of the oxazine units using a solution of the polymer in DMSO-d_6 at 60 °C and variable-temperature ^{1}H NMR spectroscopy (VT-NMR). The alkene proton resonances within the polymer backbone were compared with the diagnostic methyl signals of the oxazine isomers over the course of the experiment. Under these conditions, **poly(11)** showed no signs of degradation of the oxazine units and complete isomerization within 5 h, consistent with the equilibration time of monomer **11** (Fig. 7).

To investigate the potential for dynamic nitrosocarbonyl exchange from the polymeric system, **poly(11)** was heated at 60 °C in the presence of either oxazine **9** or **10**, each in a 2 : 1 ratio relative to oxazine repeat units in **poly(11)** (Fig. 8). After heating each mixture, the solution was added dropwise into an excess of cold methanol, causing selective precipitation of the polymeric species. In each case, ^{1}H NMR analysis of the final polymers revealed signals consistent with successful conversion of oxazine units, giving rise to **poly(9-co-11)** and **poly(10-co-11)** from the corresponding small molecule
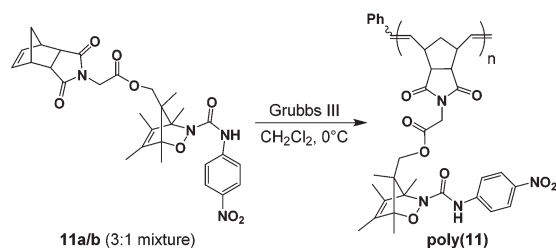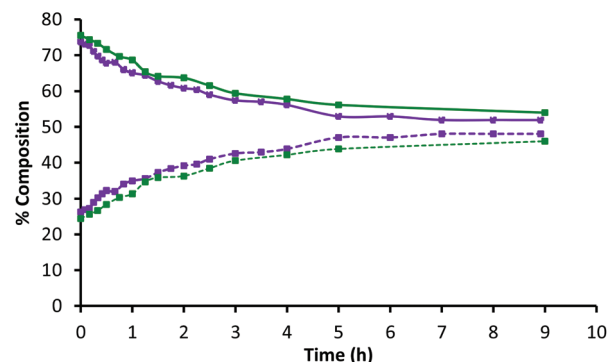

Fig. 7 Equilibration of oxazine **11** (green) and **poly(11)** (purple) in DMSO-d_6 at 60 °C. Solid line = *anti* isomer, dashed line = *syn* isomer. Percent composition refers to the ratio of *anti* and *syn* isomers.
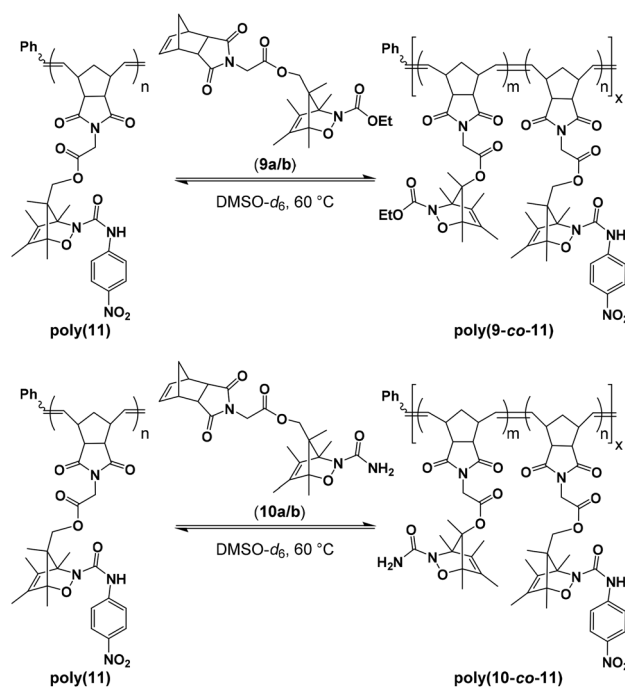

Fig. 8 Dynamic oxazine crossover between **poly(11)** and small molecule oxazines **9** and **10**. Oxazines are a mixture of *anti* and *syn* isomers; single isomer shown for simplicity.

oxazines. Each copolymer was found to have a *ca*. 2 : 1 ratio of oxazine units consistent with the initial feed ratios. These experiments confirm the ability to successfully crossover oxazine functionality with a polymeric system, and may provide opportunities for post-polymerization modifications and reversible crosslinking strategies.

Conclusions

We have investigated a series of *N*-carbonyl-substituted oxazines that display readily reversible HDA reactivity. Coincidental production of a diastereomeric mixture of each oxazine

Fig. 6 ROMP of **11** to produce **poly(11)**. Oxazines are a mixture of *anti* and *syn* isomers; single isomer shown for simplicity.

5620 | *Org. Biomol. Chem.*, 2016, **14**, 5617–5621

This journal is © The Royal Society of Chemistry 2016

provided a convenient method for comparative analysis of their dynamic nature as a function of structure and temperature. The systems appeared to be relatively robust, with dynamic equilibration and preservation of oxazine content persisting for several hours at elevated temperatures. Moreover, we found encouraging results toward incorporation of these oxazines into dynamic covalent networks and release platforms based upon polymer-oriented and hydrolysis studies. Collectively, this series of compounds displays a broad range of (retro)HDA rates and general robustness that may help to guide the design of adaptable network materials and functional polymers.

Acknowledgements

Notes and references

1 B. S. Bodner and M. J. Miller, *Angew. Chem., Int. Ed.*, 2011, **50**, 5630.

2 L. I. Palmer, C. P. Frazier and J. Read de Alaniz, *Synthesis*, 2014, 269.

3 G. W. Kirby, *Chem. Soc. Rev.*, 1977, **6**, 1.

4 G. W. Kirby and J. G. Sweeny, *J. Chem. Soc., Perkin Trans. 1*, 1981, 3250.

5 G. W. Kirby, H. McGuigan, J. W. M. Mackinnon, D. McLean and R. P. Sharma, *J. Chem. Soc., Perkin Trans. 1*, 1985, 1437.

6 J. E. T. Corrie, G. W. Kirby and J. W. M. MacKinnon, *J. Chem. Soc., Perkin Trans. 1*, 1985, 883.

7 C. C. Christie, G. W. Kirby, H. McGuigan and J. W. M. Mackinnon, *J. Chem. Soc., Perkin Trans. 1*, 1985, 2469.

8 Y. Xu, M. Alavanja, V. L. Johnson, G. Yasaki and S. B. King, *Tetrahedron Lett.*, 2000, **41**, 4265.

9 B. Zeng, J. Huang, M. W. Wright and S. B. King, *Bioorg. Med. Chem. Lett.*, 2004, **14**, 5565.

10 R. N. Atkinson, B. M. Storey and S. B. King, *Tetrahedron Lett.*, 1996, **37**, 9287.

11 Y. Adachi, H. Nakagawa, K. Matsuo, T. Suzuki and N. Miyata, *Chem. Commun.*, 2008, 5149.

12 K. Matsuo, H. Nakagawa, Y. Adachi, E. Kameda, K. Aizawa, H. Tsumoto, T. Suzuki and N. Miyata, *Chem. Pharm. Bull.*, 2012, **60**, 1055.

13 A. S. Evans, A. D. Cohen, Z. A. Gurard-Levin, N. Kebede, T. C. Celius, A. P. Miceli and J. P. Toscano, *Can. J. Chem.*, 2011, **89**, 130.

14 S. B. King, *Curr. Top. Med. Chem.*, 2005, **5**, 665.

15 A. V. Samoshin, C. J. Hawker and J. Read de Alaniz, *ACS Macro Lett.*, 2014, **3**, 753.

16 G. I. Peterson, D. C. Church, N. A. Yakelis and A. J. Boydston, *Polymer*, 2014, **55**, 5980.

17 K. K. Oehlenschlaeger, N. K. Guimard, J. Brandt, J. O. Mueller, C. Y. Lin, S. Hilf, A. Lederer, M. L. Coote, F. G. Schmidt and C. Barner-Kowollik, *Polym. Chem.*, 2013, **4**, 4348.

18 C. J. Kloxin, T. F. Scott, B. J. Adzima and C. N. Bowman, *Macromolecules*, 2010, **43**, 2643.

19 Y. Jin, C. Yu, R. J. Denman and W. Zhang, *Chem. Soc. Rev.*, 2013, **42**, 6634.

20 S. J. Rowan, S. J. Cantrill, G. R. L. Cousins, J. K. M. Sanders and J. F. Stoddart, *Angew. Chem., Int. Ed.*, 2002, **41**, 898.

21 A. Gandini, *Prog. Polym. Sci.*, 2013, **38**, 1.

22 K. M. Miranda, H. T. Nagasawa and J. P. Toscano, *Curr. Top. Med. Chem.*, 2005, **5**, 649.

23 D. A. Guthrie, A. Ho, C. G. Takahashi, A. Collins, M. Morris and J. P. Toscano, *J. Org. Chem.*, 2015, **80**, 1338.

24 D. A. Guthrie, S. Nourian, C. G. Takahashi and J. P. Toscano, *J. Org. Chem.*, 2015, **80**, 1349.

25 A. D. Sutton, M. Williamson, H. Weismiller and J. P. Toscano, *Org. Lett.*, 2012, **14**, 472.

26 D. A. Guthrie, N. Y. Kim, M. A. Siegler, C. D. Moore and J. P. Toscano, *J. Am. Chem. Soc.*, 2012, **134**, 1962.

27 R. M. Conrad and R. H. Grubbs, *Angew. Chem., Int. Ed.*, 2009, **48**, 8328.

28 C. P. Frazier, A. Bugarin, J. R. Engelking and J. Read de Alaniz, *Org. Lett.*, 2012, **14**, 3620.

29 D. Chaiyaveij, L. Cleary, A. S. Batsanov, T. B. Marder, K. J. Shea and A. Whiting, *Org. Lett.*, 2011, **13**, 3442.

30 C. P. Frazier, L. I. Palmer, A. V. Samoshin and J. Read de Alaniz, *Tetrahedron Lett.*, 2015, **56**, 3353.

31 1,4-Dicyanobenzene was used as an internal NMR standard in the trials.

32 G. E. Keck, R. R. Webb and J. B. Yates, *Tetrahedron*, 1981, **37**, 4007.

33 J. A. Love, J. P. Morgan, T. M. Trnka and R. H. Grubbs, *Angew. Chem., Int. Ed.*, 2002, **41**, 4035.